ROYAL SOCIETY
OF CHEMISTRY

PAPER

Check for updates

Coupling pretreatment of ultraviolet/ferrate (UV/Fe(VI)) for improving the ultrafiltration of natural surface water†

Fuwang Zhao[a] and Zhiwei Zhou*[b]

Ultrafiltration (UF) is a high-potential technology for purifying natural surface water; however, the problem of membrane fouling has limited its widespread application. Herein, ultraviolet (UV)–activated ferrate (Fe(VI)) was used to purify natural surface water and improve the performance of the UF membrane. The combination of UV and Fe(VI) could generate active species (Fe(V), Fe(IV), $^{\bullet}OH$ and $O_2^{\bullet-}$) to degrade pollutants, while the *in situ* produced Fe(III) had the effect of coagulation. With the above action, pollutants were removed, and the pollution load of natural surface water was reduced. After treatment with the UV/Fe(VI) system, dissolved organic carbon was reduced by 49.38%, while UV_{254} was reduced by 45.00%. The removal rate was further increased to 54.88% and 51.67% after UF treatment. In addition, the fluorescent organics were reduced by 44.22%, and the molecular weight of the organics became smaller. In the stage of UF, the terminal J/J_0 was increased from 0.61 to 0.92, and the membrane fouling resistance was decreased by 85.94%. The analysis of the membrane fouling mechanism indicates that the role of cake filtration was weakened among all the mechanisms. Fourier transform infrared spectroscopy showed that less pollutants were accumulated on the membrane surface, and scanning electron microscopy revealed that the membrane pore blockage was relieved. In summary, the UV/Fe(VI) co-treatment process proposed in this study can significantly improve the purification efficiency of the UF systems in natural surface water treatment.

1 Introduction

Ultrafiltration (UF) is considered one of the most prospective and dependable alternatives for water treatment.[1] In addition to effectively removing suspended particles and microorganisms, UF also removes colloids and some dissolved macromolecules that are more difficult to remove.[2] A major hurdle for UF in water treatment applications is membrane fouling, and this can result in increased energy consumption and even shorten the operational life of the membrane.[3,4] Natural organic matter (NOM) is one of the major membrane pollutants that can lead to serious reversible and irreversible membrane fouling.[5] In addition, the poor removal rate of low molecular weight pollutants is another obstacle to their practical use in water processing.[6]

A common method of mitigating membrane fouling is to pretreat the feed water to reduce the fouling that occurs during membrane filtration by removing pollutants or converting them to more treatable small molecule pollutants.[7–10] It is well known that oxidation processes have been reported as promising and effective pretreatment methods for mitigating NOM fouling on membranes.[11,12] Ferrate (Fe(VI)) has received increasing attention in the field of water treatment as an environmentally acceptable chemical oxidizer for the mitigation of membrane fouling.[13–16] Fe(VI) has excellent advantages for oxidizing pollutants, and nanoscale iron (hydrogen) oxides can be formed in the reduction process of Fe(VI).[17,18] They are stabilized in the treated water and can effectively react with harmful substances.[19] However, Fe(VI) is not able to act alone as an oxidant, coagulant, and disinfectant to remove some organic/inorganic pollutants.[20]

Multiple strategies for the activation of Fe(VI) have been used to produce active oxide species selectively, such as O_3, Fe(II), Fe(III), and ultraviolet (UV).[21–23] Concretely, UV radiation can activate Fe(VI), and has shown significant co-oxidation in many researches.[24,25] Generally, $^{\bullet}OH$ and $O_2^{\bullet-}$ are often regarded as active species because they are often measured in the degradation processes based on UV. In addition, UV can convert Fe(VI) to Fe(V) and Fe(IV), thus strengthening its oxidation properties.[26] It was reported that the degradation rate constant of 2,4-dichlorophenol for UV/Fe(VI) was 9.2 times higher than single Fe(VI) treatment, and it also showed greater oxidation capacity than conventional UV-based advanced oxidation processes.[5] It

[a] *School of Energy and Environment, Zhong Yuan University of Technology, Zhengzhou, 450007, China. E-mail: zhaofuwangzfw@zut.edu.cn*

[b] *College of Architecture & Civil Engineering, Faculty of Urban Construction, Beijing University of Technology, Beijing 100124, China. E-mail: zhouzw@bjut.edu.cn*

† Electronic supplementary information (ESI) available. See DOI: https://doi.org/10.1039/d3ra05582e

has also been found that UV activation can significantly enhance the removal of proteins and humic acids by Fe(VI).[27] Therefore, the UV-activated Fe(VI) strategy to enhance the effectiveness of UF is a promising approach in purifying natural surface water, but there is still a paucity of relevant studies.

In this study, a new strategy of UV-coupled Fe(VI) for enhancement of UF treatment of natural surface water is proposed. First, the effects of UV/Fe(VI) on UF influent and effluent water quality were investigated, and NOM in natural surface water was measured to elaborate the changes in the properties of contaminants during the synergetic treatment. The membrane flux, membrane resistance, and membrane fouling mechanism analysis were utilized to assess the conditions of membrane fouling, as well as interfacial characteristics including membrane morphology and functionality groups were tested. Lastly, the enhancement mechanism of UF performance was evaluated and discussed. This novel coupling strategy could provide some new insights into the improvement of effectiveness in the actual production of UF treatment of natural surface water.

2 Materials and methods

2.1 Preparation of raw water

The feed water was obtained from an artificial lake. For the experiment period, the quality of feed water indexes are: temperature = 22–25 °C, UV_{254} = 0.058–0.062 cm^{-1}, DOC = 7.2–7.9 mg L^{-1}, and pH = 6.7–7.3.

2.2 Experimental setup

As shown in Fig. 1, the experiment was divided into two phases: (1) UV/Fe(VI) pretreatment; and (2) UF processes. In the first phase, a photochemical reaction vessel with a centrally installed UV lamp (254 nm, 16 W, GPH 303T5L/4, Heraeus, Germany) was adopted. Before the experiments, the lamps were lit for at least 10 minutes to achieve a steady intensity of radiation.[28] The reaction temperature was constant at 25 ± 1 °C, controlled by the low-temperature thermostat bath (Ningbo Scientz Biotechnology Co., Ltd, China). The photochemical reactor was positioned on a magnet stirrer with a stirring speed of 150 r min^{-1}. The water sample after pre-treatment was directly used for the next stage without removing the flocs formed. During the UF phase, membranes manufactured from polyethersulfone (UP150, Microdyn-Nadir) were selected for this work. The UF equipment consists of five main components: (1) a UF cell

(dead-end filtration mode); (2) a press meter; (3) a nitrogen gas bottle (pressure maintained at 0.05 Mpa); (4) an electronic scale (automatically recorded weigh data in four-second intervals); (5) a computer equipped with data recording software. Prior to filtration, the virgin membranes were immersed in a 50% alcohol solution for 20 minutes to solubilize the organic protectant from the membranes, then they were immersed and placed in Milli-Q water. The Milli-Q water was filtered before the flux was stabilized, the flux was then calculated, followed by filtering of the 300 mL pretreated water samples. Following filtration, the Milli-Q water was then filtered at a steady flux until the fouling resistance was analyzed. During the backwash, the membrane was turned upside down, and the pressure was kept at 0.10 MPa for 2 minutes to drive 100 mL Milli-Q water across the membrane to wash away the contaminants, that had adhered to the membranes.[29]

As shown in Table S2,† it could be intuitively discovered that with the increase of UV irradiation and Fe(VI) dosage, the values of DOC showed a gradual decline. However, when the reaction conditions reached 0.06 mM Fe(VI) with 90 minutes of UV irradiation, the DOC values increased again after continuing to increase the dosage. Overall, in order to investigate the dosage effect of different agents on the mitigation effect of membrane fouling, UV/Fe(VI)-1, UV/Fe(VI)-2, and UV/Fe(VI)-3 were finally selected for the formal experiment.

Herein, the following 6 groups of sequences were set depending on the treatment methods: feed water, UV irradiation for 90 minutes (denoted as UV), 0.06 mmol L^{-1} Fe(VI) (denoted as Fe(VI)), 0.02 mmol L^{-1} Fe(VI) with 30 minutes of UV irradiation (denoted as UV/Fe(VI)-1), 0.04 mmol L^{-1} Fe(VI) with 60 minutes UV irradiation (denoted as UV/Fe(VI)-2), 0.06 mmol L^{-1} Fe(VI) with 90 minutes UV irradiation (denoted as UV/Fe(VI)-3).

2.3 Membrane fouling assessment

Changes in the specific flux (J/J_0) versus filtering volume were plotted to represent the reduction of membrane flux during UF.[30] For the purpose of better clarifying the membrane fouling, the Darcy formulation of the tandem resistance model was used to calculate the distribution of reversible and irreversible membrane fouling resistance.[31] In order to analyze the mechanism of membrane fouling, four classical membrane fouling models, namely complete blocking, standard blocking, intermediate blocking, and cake filtration, were used to fit the flux curves.[32] The specific analytical methods for membrane fouling assessment were the same as in previous studies and can be found in (Text S1†).[33–35]

2.4 Analysis methodologies

UV_{254} was measured using a UV/visible light meter (UV-1800, MAPADA), and a total organic carbon analyser (TOC-L CPH, Shimadzu) was used to determine the dissolved organic carbon (DOC). The molecular fluorescent detector (F-7100, Hitachi, Japan) was used to detect the fluorescent organic components with the following scanning parameters: excitation wavelength of 200–450 nm with a scanning spacing of 5 nm, emission wavelength of 220–550 nm with a scanning spacing of 5 nm. The
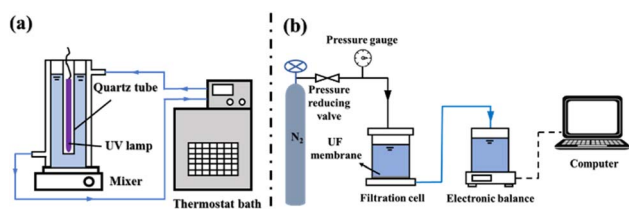

Fig. 1 Schematic of the experimental setup: (a) UV irradiation device, and (b) UF membrane filtration.

classification and quantitative calculation of fluorescent organic compounds were carried out using a reference from the previous method.[19] The molecular weight distributions of the organic compounds were determined by high-performance liquid chromatography (Waters E2695) with a UV absorbance detection (SEC-UV), and the aggregated peaks were decomposed into quantifiable Gaussian peaks using PeakFit v4.12 as shown in (Fig. S1†).[36] To determine the functional groups specific to the fouled layer, Fourier transform infrared (FTIR) spectra were analyzed using FTIR spectroscopy (Spectrum One B) and two-dimensional correlation spectroscopy (2D-COS).[37] The microscopic morphologies of the membrane interfaces were observed using a thermofield emission scanning electron microscopy (SEM, JSM-7610F Plus).

3 Results and discussion

3.1 Characteristics of NOM

3.1.1 Organics removal.
As shown in Fig. 2a, DOC was partially removed by 19.01% and 30.81% with single UV and single Fe(VI) treatments. After the synergistic treatment with UV and Fe(VI), the DOC was removed further, and the maximum

rate of removal was 49.38% after the UV/Fe(VI)-3 treatment. After filtering using the UF membrane, the removal rate was increased to 54.88%. The amount of the unsaturated organic and aromatic compounds in water samples was reflected by testing UV_{254}.[38,39] Fig. 2b demonstrates a similar pattern as DOC, where UV_{254} was not significantly removed by single UV or single Fe(VI) with removal rates of only 8.33% and 23.33%, respectively. The combined treatment improved the removal rate of UV_{254}, and the UV/Fe(VI)-3 treatment not only removed 45.00% of UV_{254} but also made the UV_{254} removal rate of UF effluent reach 51.67%. As shown in Table S3,† the association of UV with Fe(VI) promoted the production of a large number of reactive species ($^{\cdot}OH$ and $O_2^{\cdot-}$) and medium-valent iron (Fe(V) and Fe(IV)), and these highly active substances promoted the removal of DOC and UV_{254}. In addition, *in situ* generation of Fe(III) promoted coagulation and adsorption among composite systems, which was also effective in removing the pollutants.[40,41]

3.1.2 Fluorescent composition.
The fluorescent components shown in Fig. 3 were divided into five regions, representing aromatic proteins (regions I and II), fulvic acid-like substances (region III), soluble microbial product-like substances (region IV) and humic-like substances (region V), respectively.[42] The method of fluorescence area integration was used to evaluate the volume of each component, and the calculated results (Table S4 and Fig. S2†) showed that the largest proportion of substances in the raw water were aromatic proteins (55%), followed by humic-like substances (20%). Single UV treatment decreased the proportion of aromatic proteins by 8% and increased the proportion of humic-like substances by 6%. However, the proportion of aromatic proteins increased by 12%, and the proportion of humic-like substances decreased by 8% with a single Fe(VI) treatment. After the single UV or single Fe(VI) treatment, the
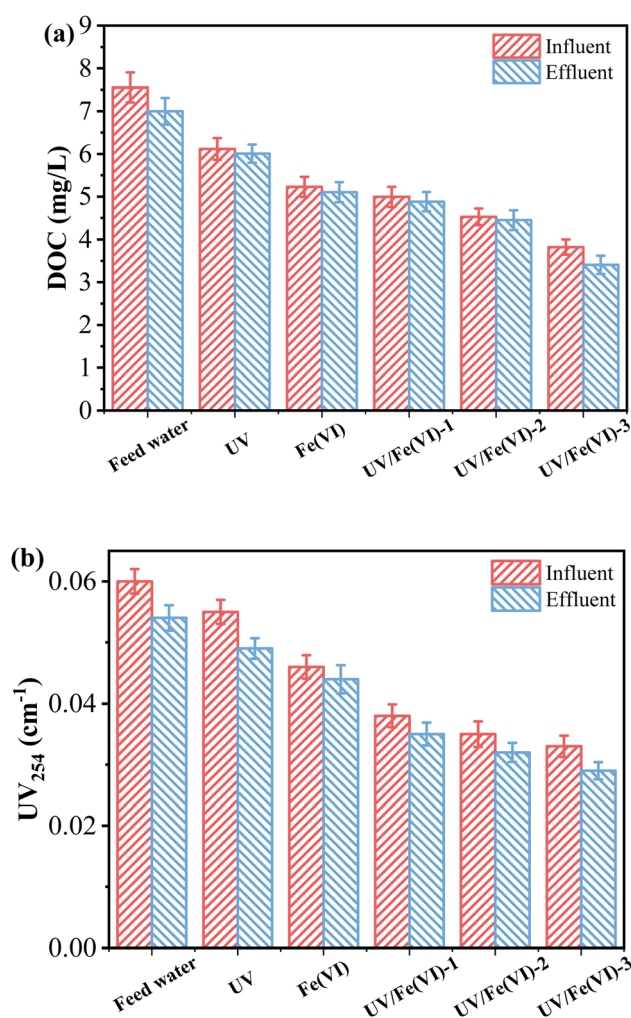

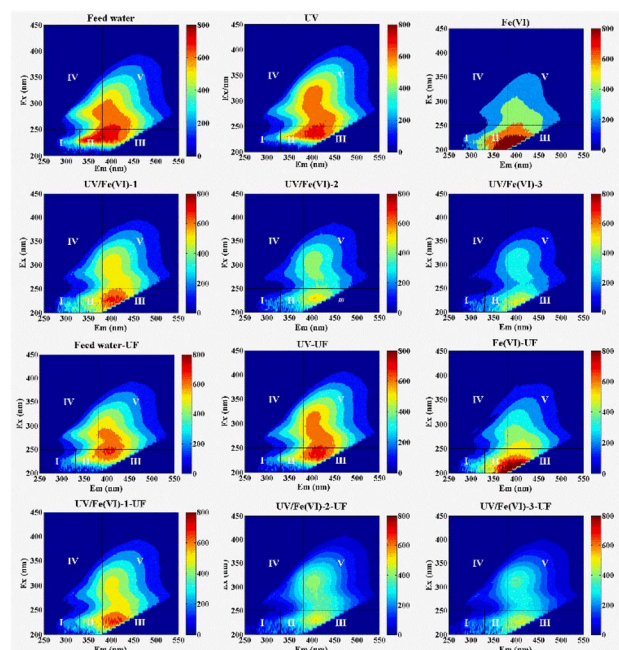**Fig. 2** Influent and effluent water quality: (a) DOC and (b) UV_{254}.

Fig. 3 Three-dimensional fluorescence spectra of influent and effluent water.

content of overall fluorescent substances barely decreased, hence it could be presumed that the fluorescent composition in the water samples was only converted and not deeply eliminated. The synergistic processing showed excellent performance in the removal of all five fluorescent substances. Although the percentage of each component varied little, the total content was significantly reduced. The total content of fluorescent substances was reduced by 9.65%, 32.91%, and 44.22% after UV/Fe(VI)-1, UV/Fe(VI)-2, and UV/Fe(VI)-3 treatments, respectively. In addition, it can be seen that the fluorescent substance content in the effluent of the UF membrane did not change much compared to that in the influent, indicating that the UF membrane did not effectively retain fluorescent substances. Overall, the synergistic effect of UV and Fe(VI) could efficiently degrade fluorescent organic compounds.

3.1.3 Distribution of molecular weight. Fig. 4 shows the molecular weight distribution of NOM. For feed water, organic matter of >2000 Da, 1500–2000 Da, 1200–1500 Da, and <1200 Da accounted for 15.03%, 34.88%, 36.77%, and 13.32% of the

NOM, respectively. Both UV and Fe(VI) have certain oxidation capacities, causing a change in the molecular weight distribution of NOM. After the single UV treatment, the percentage of organics > 2000 Da decreased to 5.74%, and the percentage of organics at 1500–2000 Da increased to 60%. The organic matter of >2000 Da disappeared, and the percentage of organic matter at 1500–2000 Da increased to 66.84% with the treatment of single Fe(VI). The Fe(VI) showed stronger oxidation after being activated by UV, and organic matter of >2000 Da had disappeared. In particular, the percentages of organic matter with 1500–2000 Da, 1200–1500 Da and <1200 Da were 50.00%, 33.37%, and 16.63% after the UV/Fe(VI)-3 treatment.

3.2 Condition of UF membrane fouling

3.2.1 Membrane flux and fouling resistance. Fig. 5 demonstrates the impact of pretreatment strategies on membrane flux and fouling resistance. As seen in Fig. 5a, the unpretreated natural water resulted in a severe reduction in the membrane flux with the J/J_0 dropping to 0.61. The mitigation of membrane fouling by single UV and Fe(VI) was inconspicuous, and the terminal J/J_0 values were only increased to 0.66 and 0.70,
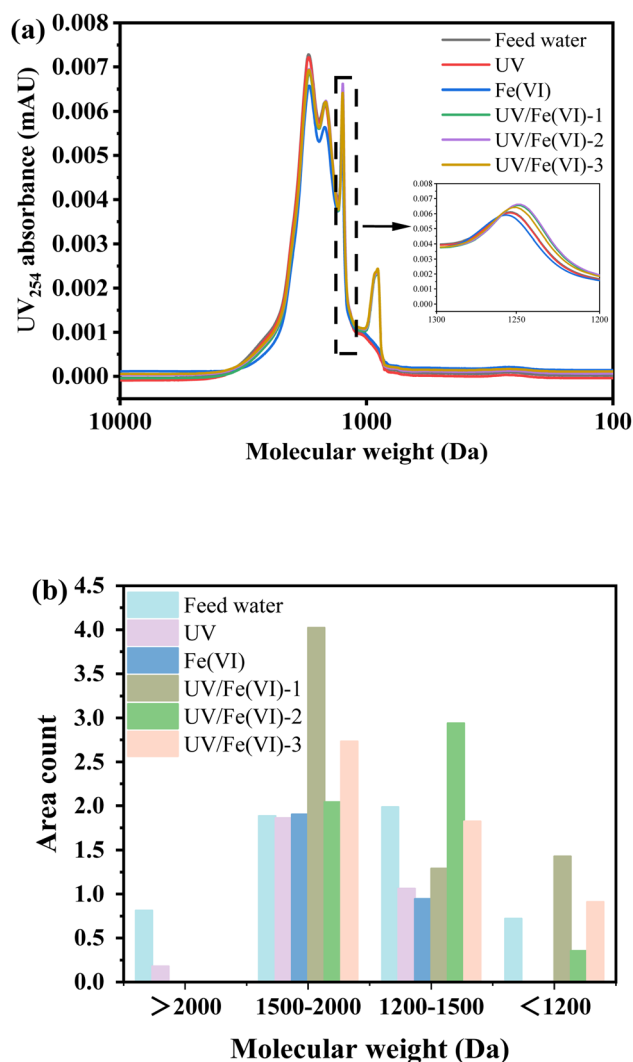

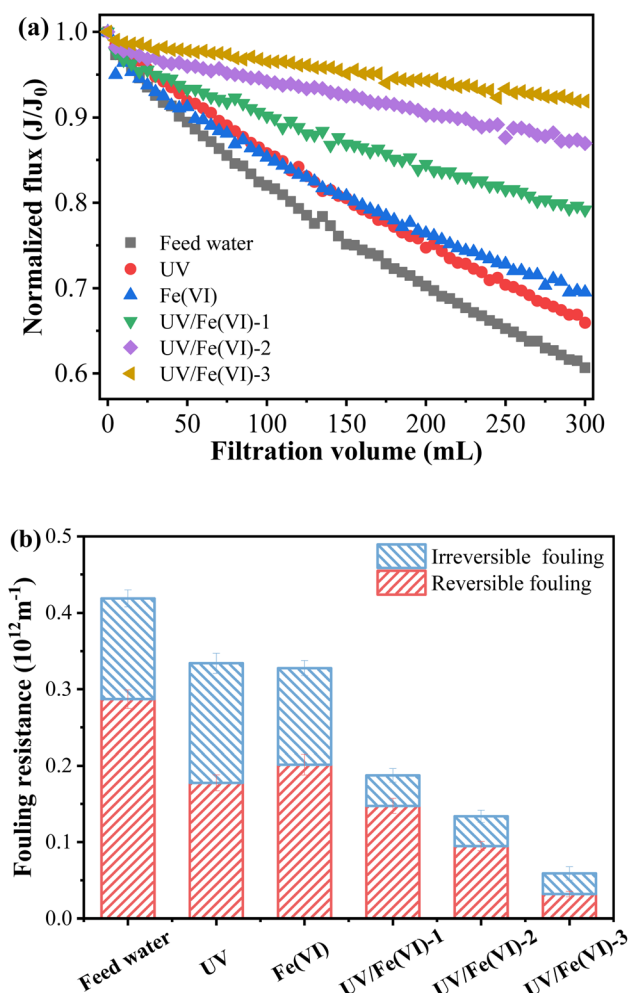Fig. 4 (a) Molecular weight distribution, and (b) change in molecular weight fractions of NOM.

Fig. 5 (a) Normalized flux (J/J_0) curves, and (b) fouling resistances of the UF membranes.

respectively. The synergistic effect of UV and Fe(VI) showed superior performance in mitigating the decrease of membrane flux. In specific terms, the terminal J/J_0 was improved to 0.79, 0.87, and 0.92 with the treatment of UV/Fe(VI)-1, UV/Fe(VI)-2 and UV/Fe(VI)-3, respectively.

As seen from Fig. 5b, the fouling resistance caused by the feed water was 0.419×10^{12} cm^{-1}, of which the reversible and irreversible fouling resistance accounted for 68.50% and 31.50%, respectively. The membrane fouling resistance was reduced by 20.29% and 21.96% after single UV and single Fe(VI) treatments, respectively, but the irreversible fouling resistance was not effectively mitigated. In particular, the single UV treatment increased the irreversible fouling resistance by 18.18%, instead. This may be due to the fact that UV oxidation alone did not significantly reduce the pollution load of natural surface water, but led to changes in the characteristics of organic pollutants. Under the coordinated action of UV and Fe(VI), both fouling resistances were effectively controlled. Not only the reversible fouling resistance was decreased by 78.61%, 70.90%, and 54.24%, but also the irreversible fouling resistance was reduced by 21.39%, 29.10%, and 45.76% after UV/Fe(VI)-1, UV/Fe(VI)-2 and UV/Fe(VI)-3 treatments, respectively. In the reaction process, Fe(VI) produced a variety of active species after being activated by UV.[24] The combined system produced reactive species such as Fe(V), Fe(IV), $^{\bullet}$OH, and $O_2^{\bullet-}$, which promoted the degradation of organic matter, and the *in situ* produced Fe(III) contributed to the reduction of membrane fouling by playing a role of coagulation and adsorption.[43]

3.2.2 Analysis of fouling mechanisms. As shown in Fig. 6, classical fouling models were used to reveal the membrane fouling mechanisms according to the methodology described in previous publications.[44,45] For the filtration of feed water, the correlation coefficients (R^2) were 0.986, 0.993, 0.997, and 0.999 for complete blocking, standard blocking, intermediate blocking, and cake filtration, respectively, indicating that all the

fouling mechanisms were involved, and the cake filtration and intermediate clogging played a primary role. The fouling mechanism changed slightly after a single UV treatment which was still dominated by cake filtration ($R^2 = 0.999$) and intermediate blocking ($R^2 = 0.999$). After a single Fe(VI) treatment, the fouling mechanism changed significantly with standard blocking ($R^2 = 1$) becoming the predominant fouling mechanism, followed by cake filtration ($R^2 = 0.997$). It indicated that single Fe(VI) treatment reduced the role of cake filtration in the composition of membrane fouling. Similar results were obtained with the treatment of UV/Fe(VI)-1, where the dominant position was taken by the standard blocking ($R^2 = 1$), followed by the cake filtration ($R^2 = 0.994$). After UV/Fe(VI)-2 and UV/Fe(VI)-3 treatments, although the standard blocking was still the dominant mechanism of action with $R^2 = 0.998$ and 0.992, the effect of cake filtration was diminished further, and the role of intermediate blocking had become the same as that of cake filtration. The UV/Fe(VI)-2 treatment resulted in an R^2 of 0.990 for both intermediate blocking and cake filtration, while the UV/Fe(VI)-3 treatment led to an R^2 of 0.988 for both intermediate blocking and cake filtration. In conclusion, the effect of cake filtration on the membrane fouling mechanism was diminished with the synergistic effect of UV and Fe(VI).

3.3 Membrane foulants characteristics

3.3.1 Surface functional groups. The functional groups of the virgin membrane and the contaminated layer at the membrane surface after filtering natural surface water were identified using FTIR, and the results are shown in Fig. 7. In addition, 2D-COS spectral pairs were applied for the further in-depth analysis, and the synchronous and asynchronous maps of the functional groups at the membrane surface after different treatment methods were obtained. After 2D-COS analysis of FTIR spectra, several characteristic peaks of pollutants were
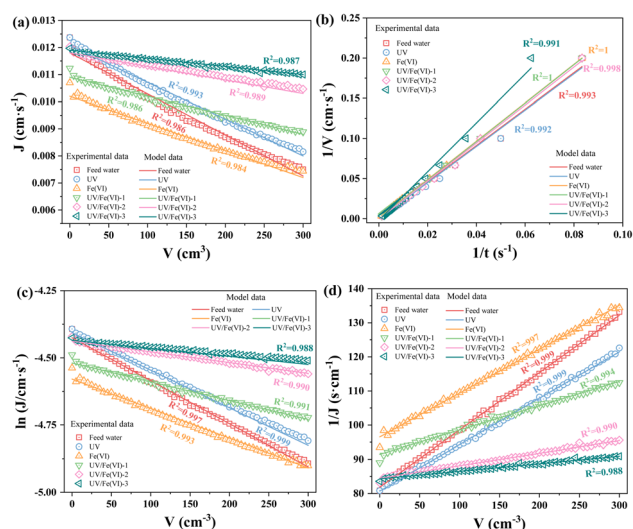
Fig. 6 Regression analyses of UF membrane fouling: (a) complete blocking, (b) standard blocking, (c) intermediate blocking, and (d) cake filtration.
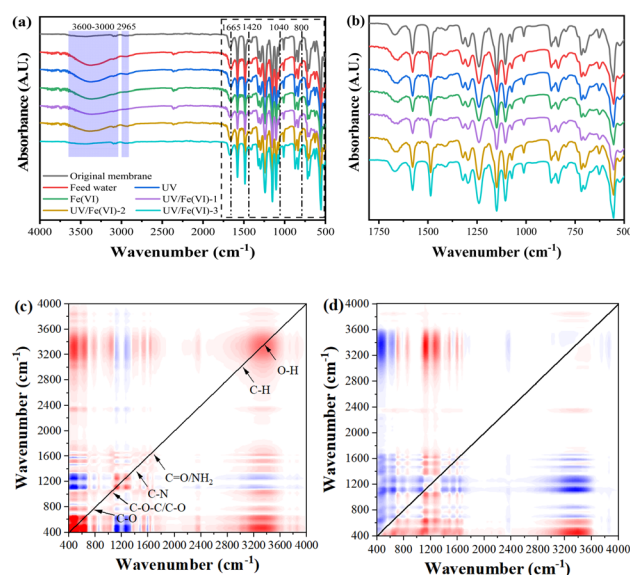
Fig. 7 (a, b) FTIR spectra, (c) synchronous and (d) asynchronous 2D-COS spectra of fouled membranes.

found at 3600–3000, 2965, 1665, 1420, 1040, and 800 cm^{-1} along the diagonal in the synchronous map. The absorbance at about 3600–3000 cm^{-1}, 1040 cm^{-1}, and 800 cm^{-1} was caused by the vibration of O–H, C–O–C/C–O, and C–O, respectively, and these three functional groups proved the existence of carbohydrates.[46,47] Peaks at 1665 cm^{-1} and 1420 cm^{-1} were signatures of C=O/NH$_2$ and C–N, both indicating the existence of protein components.[48] The peak at 2965 cm^{-1} was the signature sign of C–H binding among humic acid.[49] It can be concluded that the pollutants adhering to the membrane surface were mainly carbohydrates, protein-like substances, and humic acids. As can be seen from FTIR spectra, the signature absorbance peaks for those pollutants were reduced to varying degrees after UV/Fe(vi) treatment, indicating that the pollutants on the membrane surface were decreased.

The degree of functional groups affected by pretreatment can be further seen by the synchronous map. As depicted in Fig. 7c, the higher peak intensities in the map suggest that the appropriate functional groups are more influenced by the pretreatment method. From the peak intensities in the synchronous map, the order O–H > C–O–C/C–O > C–H > C=O/NH$_2$ > C–N > C–O is presented, suggesting that O–H was most affected by the pretreatment, followed by C–O–C/C–O. The contrast between the synchronous and asynchronous plots also showed the sequential variation of the functional groups in the FTIR spectra under various treatments.[50] Table S5† summarizes the signals of the synchronous and asynchronous maps of each functional group, and the following order can be deduced: C–H > O–H > C–O–C/C–O > C–O > C–N > C=O/NH$_2$. In conclusion, UV/Fe(vi) treatment was very effective in controlling the cumulation of organics on the surface of the membrane.

3.3.2 Surface morphology. To better investigate the performance of UV/Fe(vi) treatment in controlling membrane fouling, the morphology of UF membranes was observed by SEM, as shown in Fig. 8. It can be visualized from Fig. S3† that the surface structure of the virgin membrane was glossy with high porosity, and the distribution of the membrane pores was uniform. It could be intuitively seen from Fig. 8a that after the filtration of raw water, macromolecular organics accumulated on the surface of the UF membrane and formed a dense cake layer, while small molecular organics would enter the

membrane pore and cause severe pore blockage. The membrane surface morphology changed slightly after the UV treatment alone, and the surface of the membrane remained coated with large amounts of contaminants. With single Fe(vi) treatment, a lot of flocs accumulated on the membrane surface, and the volume of the contaminants became smaller. This was due to the oxidation of large molecules into small molecules by Fe(vi), and the capture of pollutants by the *in situ* generation of iron flocs. The surface morphology of the membrane after UV/Fe(vi)-1 treatment was similar to the single Fe(vi), while the number of pollutants on the membrane surface was significantly reduced after UV/Fe(vi)-2 and UV/Fe(vi)-3 treatments. Especially for the UV/Fe(vi)-3 treatment, the membrane pores on the surface were clearly visible, accompanied by a significant increase in porosity and membrane flux. The results mentioned above further validated the efficacy of the UV/Fe(vi) process, which significantly reduced the contaminants accumulated on the surface and controlled the fouling of the membrane.

4 Conclusions

Herein, a UV/Fe(vi)-enhanced UF process for the treatment of natural surface water is proposed. The effects and mechanisms of membrane fouling mitigation and water purification effectiveness were investigated by characterization of NOM, membrane fouling, and membrane interface properties. The results showed that the pollutants in water were efficiently eliminated by the synergistic effect of UV and Fe(vi) with removal rates of 49.38%, 45.00%, and 44.22% for DOC, UV$_{254}$, and fluorescent organics, respectively. The Fe(vi) exerted outstanding oxidation ability after being activated by UV, and oxidized large-molecule organics to small-molecule organics. Active species such as Fe(v), Fe(iv), $^{\bullet}$OH, and O$_2^{\bullet-}$ were produced after Fe(vi) was activated by UV, which promoted the decomposition of the organic matter. The Fe(iii) generated *in situ* played a role in the coagulation and adsorption, which also contributed to the reduction of pollutants. In the stage of UF, the terminal J/J_0 was increased from 0.61 to 0.92, and the membrane fouling resistance was decreased by 85.94%, among which the reversible and irreversible fouling resistances were decreased by 54.24% and 45.76%, respectively. The analysis of the membrane fouling mechanism showed that UV/Fe(vi) treatment reduced the role of cake filtration. FTIR and SEM results suggested that the pollutants cumulated on the membrane surface were decreased, and the membrane pore-blocking phenomenon was alleviated. In conclusion, the coupled strategy of UV and Fe(vi) has potential applications in the pretreatment of natural surface water and the enhancement of UF performance.

Author contributions

Fuwang Zhao: investigation, methodology, writing – original draft.

Conflicts of interest
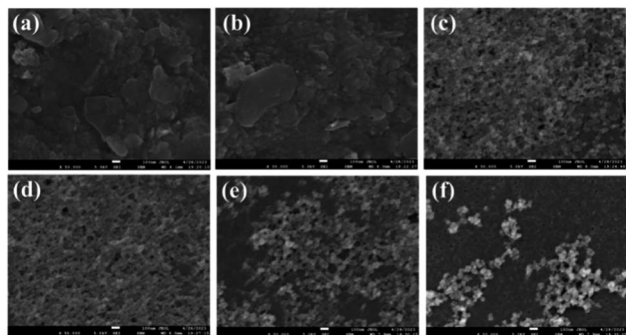
There are no conflicts of interest to declare.

Fig. 8 SEM images of the membranes fouled by the feed water (a) without pretreatment, and pretreated by (b) UV, (c) Fe(vi), (d) UV/Fe(vi)-1, (e) UV/Fe(vi)-2, and (f) UV/Fe(vi)-3 (500 00× magnification).

Acknowledgements

References

1 A. Ding, Z. Ren, Y. Zhang, J. Ma, L. Bai, B. Wang and X. Cheng, *Chemosphere*, 2021, **285**, 131459.

2 W. Song, Z. Gao, C. Hou, X. Cheng, J. Lian, T. Yang, Z. Zhou, D. Wu and H. Liang, *Sci. Total Environ.*, 2023, **888**, 164235.

3 W. Yu, D. Zhang and N. J. D. Graham, *Water Res.*, 2017, **120**, 146–155.

4 X. Cheng, Y. Zhang, Q. Fan, L. Wang, S. Shi, X. Luo, X. Zhu, D. Wu and H. Liang, *Chem. Eng. J.*, 2023, **454**, 140450.

5 S. Wu, H. Liu, Y. Lin, C. Yang, W. Lou, J. Sun, C. Du, D. Zhang, L. Nie, K. Yin and Y. Zhong, *Chemosphere*, 2020, **244**, 125490.

6 B. Liu, J. Yin, J. Wu, X. Cheng, K. Yang, G. Li and Z. Shi, *J. Water Process. Eng.*, 2022, **49**, 103156.

7 A. Ding, Z. Ren, L. Hu, R. Zhang, H. H. Ngo, D. Lv, J. Nan, G. Li and J. Ma, *Sci. Total Environ.*, 2022, **850**, 157986.

8 Z. Chen, B. Yang, Q. Wen and Y. Tang, *Chemosphere*, 2021, **274**, 129862.

9 Y. Wan, P. Xie, Z. Wang, J. Wang, J. Ding, R. Dewil and B. Van der Bruggen, *Chemosphere*, 2021, **263**, 127993.

10 J. Xing, H. Liang, C. J. Chuah, Y. Bao, X. Luo, T. Wang, J. Wang, G. Li and S. A. Snyder, *Water Res.*, 2019, **167**, 115112.

11 Q. Fan, X. Cheng, X. Zhu, C. Luo, H. Ren, D. Wu and H. Liang, *Sep. Purif. Technol.*, 2022, **287**, 120579.

12 W. Liu, C. Zhao, S. Zhou, B. Liu, X. Cheng, Z. Xue and T. Zhu, *Water Res.*, 2022, **223**, 119025.

13 H. Y. He, W. Qiu, Y. L. Liu, H. R. Yu, L. Wang and J. Ma, *Water Res.*, 2021, **190**, 116690.

14 J. Lian, L. Zhang, F. Tan, J. Xu, R. Mu, D. Wu, H. Liang and X. Cheng, *Chemosphere*, 2022, **308**, 136377.

15 Y. Jin, P. Li, B. Xu, L. Wang, G. Ma, S. Chen, F. Tan, Y. Shao, L. Zhang, Z. Yang, F. Chen, W. Li, X. Cheng and D. Wu, *J. Cleaner Prod.*, 2022, **342**, 130947.

16 Y. Zhu, J. Nie, X. Yang and X. Guan, *J. Hazard. Mater.*, 2021, **412**, 125297.

17 L. Hu, M. A. Page, T. Sigstam, T. Kohn, B. J. Mariñas and T. J. Strathmann, *Environ. Sci. Technol.*, 2012, **46**, 12079–12087.

18 R. Prucek, J. Tuček, J. Kolařík, I. Hušková, J. Filip, R. S. Varma, V. K. Sharma and R. Zbořil, *Environ. Sci. Technol.*, 2015, **49**, 2319–2327.

19 J. Liu, K. He, S. Tang, T. Wang and Z. Zhang, *Sep. Purif. Technol.*, 2019, **217**, 118–127.

20 T. He, B. Zhou, H. Chen and R. Yuan, *J. Environ. Chem. Eng.*, 2022, **10**, 108706.

21 Q. Han, W. Dong, H. Wang, H. Ma, Y. Gu and Y. Tian, *RSC Adv.*, 2019, **9**, 41783–41793.

22 X. Zhang, M. Feng, C. Luo, N. Nesnas, C.-H. Huang and V. K. Sharma, *Environ. Sci. Technol.*, 2021, **55**, 623–633.

23 Y. Chen, M. Xiao, Z. Wang, W. Jiang, Y. Guo and Z. Liu, *Desalin. Water Treat.*, 2016, **57**, 12882–12890.

24 H. Aslani, S. Nasseri, R. Nabizadeh, A. Mesdaghinia, M. Alimohammadi and S. Nazmara, *J. Environ. Manage.*, 2017, **203**, 218–228.

25 Y. Chen, Y. Xiong, Z. Wang, Y. Chen, G. Chen and Z. Liu, *Desalin. Water Treat.*, 2015, **55**, 506–513.

26 T. Yang, J. Mai, H. Cheng, M. Zhu, S. Wu, L. Tang, P. Liang, J. Jia and J. Ma, *Environ. Sci. Technol.*, 2022, **56**, 1221–1232.

27 J. Wang, Y. Liu, L. Feng, Y. Wang and H. Jia, *J. Water Process. Eng.*, 2022, **49**, 103183.

28 Z. Wang, Y. Wan, P. Xie, A. Zhou, J. Ding, J. Wang, L. Zhang, S. Wang and T. C. Zhang, *Chemosphere*, 2019, **214**, 136–147.

29 W. Song, Z. Gao, F. Tan, X. Cheng, T. Yang, D. Wu, J. Yang and H. Liang, *Chemosphere*, 2023, **333**, 138956.

30 Z. Ren, X. Cheng, P. Li, C. Luo, F. Tan, W. Zhou, W. Liu, L. Zheng and D. Wu, *Sci. Total Environ.*, 2020, **739**, 140030.

31 X. Cheng, J. Lian, Z. Ren, C. Hou, Y. Jin, L. Zhang, X. Zhu, C. Luo, D. Wu and H. Liang, *Water Res.*, 2021, **204**, 117622.

32 Y. Shen, W. Zhao, K. Xiao and X. Huang, *J. Membr. Sci.*, 2010, **346**, 187–193.

33 X. Cheng, P. Li, W. Zhou, D. Wu, C. Luo, W. Liu, Z. Ren and H. Liang, *Chemosphere*, 2019, **221**, 812–823.

34 L. Yun, Z. Gao, X. Cheng, P. Li, L. Wang, N. Guo, C. Luo, X. Zhu, B. Liu, D. Wu and H. Liang, *Chemosphere*, 2022, 135037.

35 X. Cheng, D. Wu, H. Liang, X. Zhu, X. Tang, Z. Gan, J. Xing, X. Luo and G. Li, *Water Res.*, 2018, **145**, 39–49.

36 S. R. Sarathy and M. Mohseni, *Environ. Sci. Technol.*, 2007, **41**, 8315–8320.

37 J. Wang, Q. Liu, L. Xu, M. S. Siddique and W. Yu, *Sep. Purif. Technol.*, 2023, **314**, 123611.

38 J. Altmann, L. Massa, A. Sperlich, R. Gnirss and M. Jekel, *Water Res.*, 2016, **94**, 240–245.

39 U. von Gunten, *Water Res.*, 2003, **37**, 1443–1467.

40 J. Lian, X. Cheng, X. Zhu, X. Luo, J. Xu, F. Tan, D. Wu and H. Liang, *Sci. Total Environ.*, 2023, **858**, 159893.

41 H. He, Y. Liu, L. Wang, W. Qiu, D. Li, Z. Liu and J. Ma, *Water Res.*, 2023, **229**, 119520.

42 J. Liu, K. He, J. Zhang, C. Li and Z. Zhang, *J. Membr. Sci.*, 2019, **590**, 117310.

43 A. Talaiekhozani, M. Salari, M. R. Talaei, M. Bagheri and Z. Eskandari, *J. Environ. Manage.*, 2016, **184**, 204–209.

44 F. Qu, H. Liang, J. Zhou, J. Nan, S. Shao, J. Zhang and G. Li, *J. Membr. Sci.*, 2014, **449**, 58–66.

45 W. R. Bowen, J. I. Calvo and A. Hernández, *J. Membr. Sci.*, 1995, **101**, 153–165.

46 M. B. M. Y. Ang, G.-W. Huang, M.-Y. Chu, J. C. Millare, S.-H. Huang and K.-R. Lee, *J. Water Process. Eng.*, 2022, **48**, 102843.

47 Y.-T. Chiou, M.-L. Hsieh and H.-H. Yeh, *Desalination*, 2010, **250**, 648–652.

48 J. Lian, X. Cheng, X. Zhu, X. Luo, J. Xu, F. Tan, D. Wu and H. Liang, *Sci. Total Environ.*, 2022, 159893.

49 X. Cheng, C. Hou, H. Gao, P. Li, X. Zhu, C. Luo, L. Zhang, Y. Jin, D. Wu and H. Liang, *Water Res.*, 2022, **211**, 118067.

50 Y. Park, S. Jin, I. Noda and Y. M. Jung, *J. Mol. Struct.*, 2020, **1217**, 128405.